Journal of Power Sources 196 (2011) 7951–7956

Contents lists available at ScienceDirect

Journal of Power Sources

journal homepage: www.elsevier.com/locate/jpowsour

Codeposited PtSb/C catalysts for direct formic acid fuel cells

Xingwen Yu, Peter G. Pickup*

Department of Chemistry, Memorial University of Newfoundland, St. John's, Newfoundland, Canada A1B 3X7

ARTICLE INFO

Article history:
Received 18 February 2011
Received in revised form 13 May 2011
Accepted 19 May 2011
Available online 27 May 2011

Keywords:
Direct formic acid fuel cell (DFAFC)
PtSb/C catalyst
Codeposition
Catalytic activity

ABSTRACT

Carbon supported PtSb catalysts were synthesized by codeposition of platinum and antimony on Vulcan® carbon black. X-ray diffraction (XRD) analysis revealed that the Sb was alloyed with the Pt while XPS indicated that a large fraction of the Sb was in an oxidized state, with only partial alloying. The performances of catalysts with a range of compositions were compared in a multi-anode direct formic acid fuel cell (DFAFC). A 0.29 mol fraction of Sb was found to provide the best performance with a maximum specific power output of 280 W g^{-1} Pt. CO stripping results indicated that the addition of Sb at this optimum level greatly suppressed both CO adsorption and H adsorption/desorption, as well as promoting oxidative stripping of CO. The results are compared with those for previously studied catalysts prepared by the reductive deposition of Sb on a carbon supported Pt catalyst.

1. Introduction

Due to a number of advantages over direct methanol fuel cells, direct formic acid fuel cell (DFAFC) systems are attracting considerable attention and being developed for portable power applications [1]. Pt based anode catalysts currently offer the best long term performance and there is a long history of fundamental studies of formic acid oxidation at Pt based electrodes. In particular, the effects of foreign adatoms on Pt have attracted considerable attention because of the insight that they have provided into the mechanism of formic acid electrooxidation [2,3]. These studies have indicated that enhancement of formic acid oxidation by a second metal can occur through a bi-functional effect in which oxygen species on the second metal combine with CO adsorbed on Pt sites [4], a third body or ensemble effect in which atoms of the second metal prevent CO formation by decreasing the number of adjacent Pt sites on the catalyst surface [2] and/or electronic ligand effects in which the second metal changes the electronic structure of the Pt surface [2].

The knowledge gained from fundamental studies has been increasingly applied to the development of anode catalysts for DFAFCs as this technology has developed. The addition of less noble metal to Pt, such as Ru [5–7], Pd [5,8,9], Au [6], Bi [7,10–14], Pb [11,12,15–22], As [10], Sn [11] and Sb [3,11,22–25], has been shown to decrease the formic acid oxidation overpotential. PtSb is one of the most effective anode catalyst systems for DFAFCs [22], and the mechanistic details have been recently discussed [3]. An unsupported intermetallic PtSb catalyst [11], an unsupported decorated PtSb catalyst prepared by underpotential deposition (upd) [24], and carbon supported PtSb/C catalysts prepared by chemical deposition of Sb on the surface of a commercial 40% Pt/C catalyst [22] have been employed in DFAFCs.

Although deposition of Sb on Pt (decoration) provides very active catalysts, it is not clear whether this is the most effective methodology. Optimum activities were found to occur at high Sb coverages (ca. 70% of the Pt surface) [22], which suggest that a large fraction of the Pt may not be effectively utilized. In this paper, we report on PtSb/C catalysts prepared by codeposition of Pt and Sb on Vulcan® carbon black, and compare their characteristics and DFAFC performances with those of previously reported [22] catalysts prepared by the decoration of Pt/C. The results provide considerable insight into the multiple roles that Sb can play during formic acid oxidation at PtSb catalysts.

2. Experimental

2.1. Preparation of PtSb/C catalysts

Vulcan XC-72® carbon black (200 mg) was conditioned by stirring in 10 M HNO_3 in deionised (DI) water for 12 h and then rinsing with water until the pH reached 6–7. The pretreated carbon black was added to a solution prepared with 2 mL of 5 g L^{-1} polyvinyl alcohol (PVA), 25 mL of 10 g L^{-1} H_3BO_3, 10 mL of 5 g L^{-1} NH_4F, K_2PtCl_4 (5 g L^{-1} dissolved in 5 M HCl) and $SbCl_3$ (5 g L^{-1} dissolved in 5 M HCl), and diluted to 1 L with DI water. The quantities of the K_2PtCl_4 and $SbCl_3$ solutions were selected to provide a 40% metal loading on the carbon support and the targeted Pt:Sb ratios listed in Table 1. The mixture was stirred vigorously while 50 mL of freshly

* Corresponding author. Tel.: +1 709 864 8657; fax: +1 709 864 3702.
E-mail address: ppickup@mun.ca (P.G. Pickup).

0378-7753/$ – see front matter © 2011 Elsevier B.V. All rights reserved.
doi:10.1016/j.jpowsour.2011.05.051

Table 1
Metal loadings and ratios for the PtSb/C catalysts from EDX and TGA, and mean crystallite sizes from XRD.

	Target Pt:Sb mass ratio (Sb mole fraction)	Pt:Sb mass ratio from EDX	Total metal loading from TGA	Pt (%)	Sb (%)	Crystallite size (nm)
PtSb(2:1)/C	2:1 (0.44)	2.1:1	39.4%	26.7	12.7	1.4
PtSb(3:1)/C	3:1 (0.35)	3.0:1	41.7%	31.3	10.4	1.6
PtSb(4:1)/C	4:1 (0.29)	4.2:1	41.6%	33.6	8.0	1.8
PtSb(5:1)/C	5:1 (0.24)	5.0:1	41.5%	34.6	6.9	2.1
PtSb(6:1)/C	6:1 (0.21)	6.2:1	41.7%	35.9	5.8	2.2
PtSb(8:1)/C	8:1 (0.17)	8.1:1	42.2%	37.6	4.6	2.7

prepared 0.1 M $NaBH_4$ was added drop-wise, followed by raising the pH to 9–10 by addition of 5 M NaOH. The solution was stirred vigorously for 1 h, after which the catalyst was allowed to settle for 30 min. The product was collected by filtration, rinsed with DI water and dried at 80 °C for 8 h under vacuum. Preparation of the Sb decorated Pt/C catalysts has been described previously [22].

2.2. Fuel cell performance tests

Electrodes for fuel cell performance tests were prepared by depositing the catalysts onto carbon fiber paper (Toray TGP-H-090) as follows. The catalyst was first dispersed in a mixture of DI water and Nafion solution® (DuPont; 5% Nafion, 30–60% propyl alcohols, 30–60% water), then the resulting slurry was spread onto the carbon fiber paper and dried in the air. The loading of the catalyst was maintained at 1.6 mg cm^{-2} (including the carbon support and Nafion), and the ratio of net Nafion to the catalyst was 1:4 (w/w). The Pt loading ranged from 0.34 to 0.51 mg cm^{-2}, depending on the Pt:Sb ratio. Commercial 40% HP™ Pt on Vulcan XC-72® carbon black from BASF® was also used for comparison.

Evaluation of the catalysts was performed in a multi-anode DFAFC [26]. Anode array membrane electrode assemblies (MEA) were prepared with a 5 cm^2 cathode (consisting of Pt black on carbon fiber paper) and nine (3 × 3 array) 0.23 cm^2 anodes which were hot pressed (135 °C, 100 kg cm^{-2}, 3 min) onto either side of a Nafion 115® membrane. The multi-anode DFAFC was operated with a multi-channel potentiostat (Arbin®). The anode fuel used was 5 M formic acid (puriss. p.a., ACS reagent, reag. Ph. Eur. 98+%) at a flow rate of 0.2 mL min^{-1}. At the cathode, oxygen was supplied at a flow rate of 100 sccm. The multi-anode DFAFC was operated at ambient temperature.

Polarization plots were obtained in a voltage staircase mode in which the voltage applied to the cell was stepped from the open circuit voltage (OCV) to a final voltage of 0.1 V in 15 mV intervals. The current was allowed to stabilize for 30 s at each cell voltage.

2.3. CO-stripping experiments

CO stripping cyclic voltammograms (CV) were acquired in a conventional three-electrode electrochemical cell by saturating the solution with CO for 30 min with the working electrode at open circuit, then purging the cell with nitrogen for 15 min and acquiring the CV. The working electrode was prepared as described in Section 2.2, by depositing 1.6 mg of the catalyst (including carbon support and Nafion) onto 1 cm^2 of a strip of carbon fiber paper. A Pt wire counter electrode, Hg/Hg_2SO_4 reference electrode and 0.5 M H_2SO_4 (aq) electrolyte were used.

2.4. Characterization of the catalysts

Thermogravimetric analysis (TGA) was performed with a TA Instruments Q500 TGA analyzer. Energy dispersive X-ray spectra (EDX) were obtained with a Bruker Xflash 4010 SDD energy dispersive X-ray analyzer. X-ray diffraction (XRD) data was acquired with a Rigaku Ultima IV (with standard attachment) X-ray diffractometer using a Cu Kα source (λ = 0.15418 nm). The scan range was from 20° to 100°. X-ray photoelectron spectra (XPS) were obtained with a Multilab 3000 XPS system (Dalhousie University).

3. Results

3.1. Characterization of the catalysts

The compositions of the PtSb/C catalysts were determined by EDX and TGA. Pt:Sb mass ratios determined by EDX are summarized in Table 1, where it can been seen that the measured ratios are closed to the targeted values. The total metal loadings (Pt + Sb) on the carbon support were determined by TGA, where each catalyst was heated to 800 °C until the carbon support was totally burned off. The residual mass was attributed to Pt and Sb_2O_3. The total metal loadings (Table 1) were close to the targeted value of 40%.

XRD patterns for the PtSb/C catalysts and a commercial Pt/C catalyst are shown in Fig. 1. The main Pt peaks at 39.8° (Pt 1 1 1), 46.2° (Pt 2 0 0), 67.5° (Pt 2 2 0) and 81.3° (Pt 3 1 1) can be clearly seen for the PtSb(5:1)/C, PtSb(6:1)/C, PtSb(8:1)/C and Pt/C catalysts (Fig. 1d, e, f and g). However, for the highest Sb contents (PtSb(2:1)/C, PtSb(3:1)/C and PtSb(4:1)/C), only the Pt 111 (39.8°) peak can be clearly observed. It should also be noted that no Sb

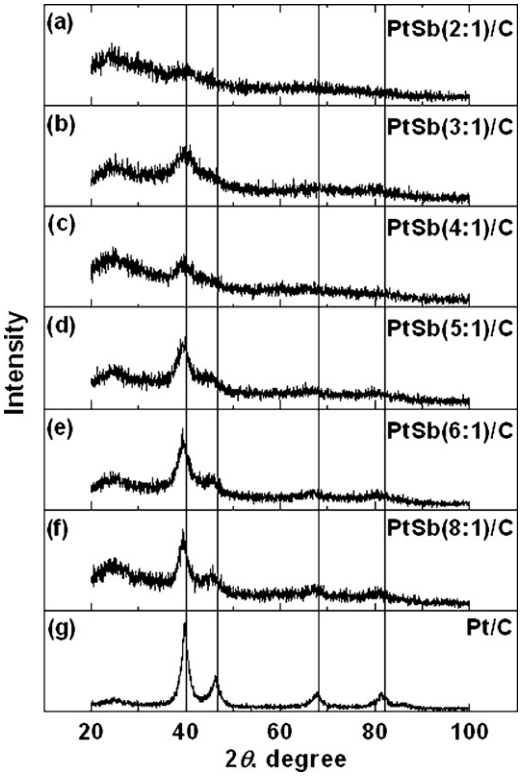

Fig. 1. XRD patterns of the (a) PtSb(2:1)/C, (b) PtSb(3:1)/C, (c) PtSb(4:1)/C, (d) PtSb(5:1)/C, (e) PtSb(6:1)/C, (f) PtSb(8:1)/C and (g) Pt/C catalysts.

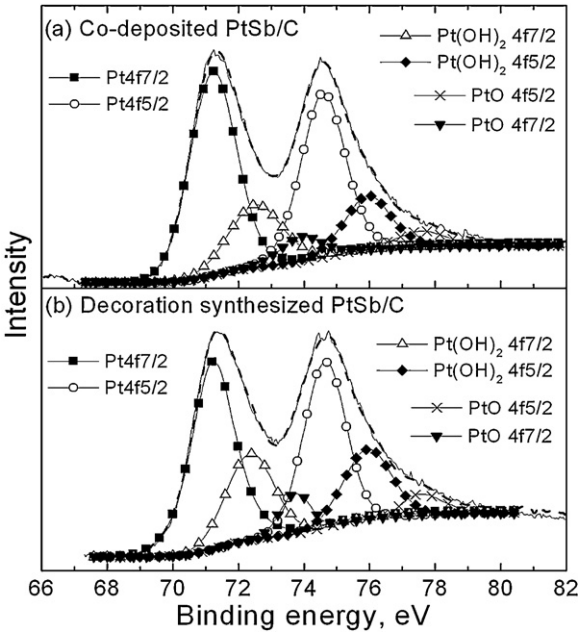

Fig. 2. Pt 4f XPS spectra of (a) the codeposited PtSb(4:1)/C catalyst and (b) a PtSb(3:1)/C catalyst prepared by deposition of Sb on commercial Pt/C [22].

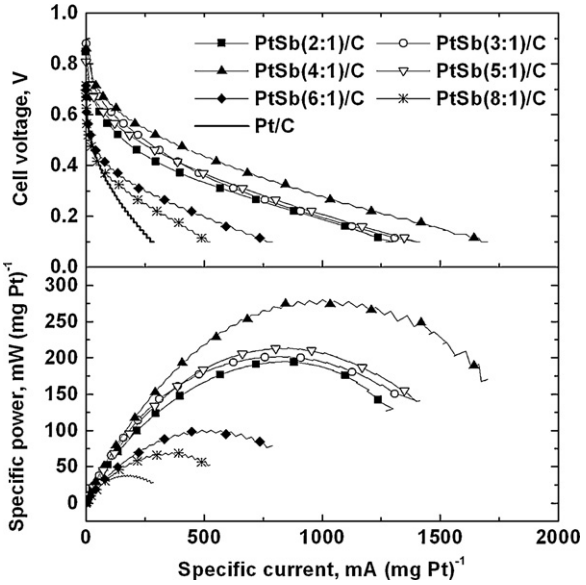

Fig. 4. Polarization curves and power plots (averaged from three electrodes for each catalyst) for multi-anode DFAFCs with PtSb(2:1)/C (MEA#1), PtSb(3:1)/C (MEA#1), PtSb(4:1)/C (MEA#1), PtSb(5:1)/C (MEA#2), PtSb(6:1)/C (MEA#2), PtSb(8:1)/C (MEA#2) and Pt/C [22] anode catalysts.

peaks can be observed in any of the spectra, which suggests that the Sb was alloyed with Pt. This is verified for the PtSb(4:1)/C, PtSb(5:1)/C, PtSb(6:1)/C, PtSb(8:1)/C catalysts by the shifts of the Pt peaks relative to the positions for the Pt/C (peak shifts were not observed for the Sb decorated Pt/C catalysts [22]). The Pt 1 1 1 (at 39.8°) peaks were very broad for the PtSb(2:1)/C and PtSb(3:1)/C catalysts, indicating more amorphous structures with very small Pt crystallites. Mean particle sizes determined from the XRD data are presented in Table 1. They ranged from 1.4 nm to 2.7 nm and increased with increasing Pt:Sb ratio.

XPS was performed on the PtSb(4:1)/C catalyst (Figs. 2 and 3 for Pt and Sb, respectively). The main Pt 4f peaks (Fig. 3a) at 71.23 eV and 74.58 eV can be attributed to metallic Pt(0), while the asymmetry indicates the presence of surface oxides. There are very similar spectra in the literature for commercial Pt/C catalysts [27]. For comparison, the Pt 4f spectrum of a PtSb(3:1)/catalyst prepared by deposition of Sb on a commercial Pt/C electrode [22] is shown in Fig. 2b. There are not significant differences in the Pt 4f region of the spectra between the two types of PtSb/C catalyst.

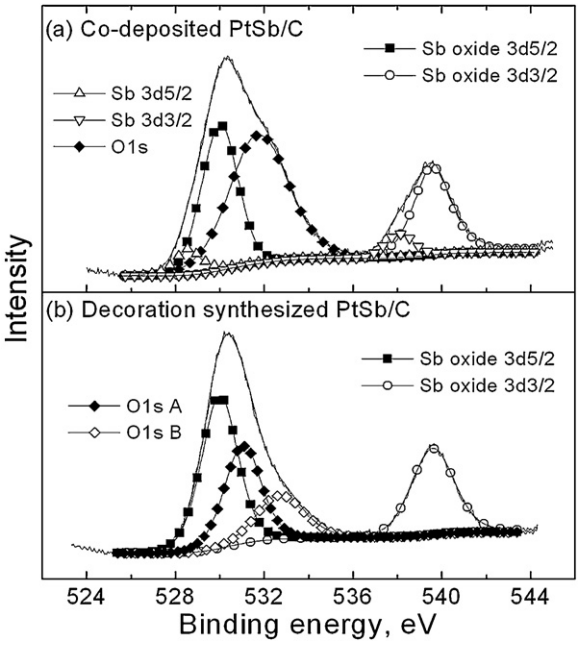

Fig. 3. Sb 3d and O 1s XPS spectra of (a) the codeposited PtSb(4:1)/C catalyst and (b) a PtSb(3:1)/C catalyst prepared by deposition of Sb on commercial Pt/C [22].

Fig. 3a shows overlapping high resolution Sb 3d and O 1s spectra for the codeposited PtSb(4:1)/C catalyst. The binding energies of the main Sb peaks at 530.0 eV (3d5/2) and 539.6 eV (3d3/2) indicate that the Sb was present as Sb oxide species, and mainly as Sb_2O_3 [22,24]. However, small secondary signals at 528.6 eV and 538.1 eV do suggest the presence of Sb(0) which would be consistent with alloying of some of the Sb with Pt, with the bulk of the Sb present as surface oxides. In contrast, a catalyst prepared by deposition of Sb on a commercial Pt/C electrode [22] showed no evidence of Sb(0) (Fig. 3b).

The O 1s spectra for the codeposited PtSb(4:1)/C and Sb decorated Pt/C catalysts were clearly different (Fig. 3). The signal for the codeposited PtSb(4:1)/C clearly extended to higher energies, and could be simulated with a single peak at 531.6 eV. In contrast, the signal for the Sb decorated Pt/C appears to represent a main peak at 531.0 eV with a minor component at 532.6 eV. Since both Pt and Sb oxides were shown to be present in the samples by the Pt 4f and Sb 3d spectra, these results imply greater overlap of the Pt–O and Sb–O signals for the codeposited PtSb(4:1)/C, which would be consistent with the other evidence for partial alloying of the Pt and Sb.

3.2. Fuel cell performances

Cell performances of the PtSb/C catalysts and the commercial Pt/C catalyst were compared in a multi-anode DFAFC by use of anode array membrane electrode assemblies (MEAs). In order to minimize and quantify the effects of variations between experiments, the array MEAs were prepared with three electrodes of each type of catalyst, and average results for each set of three electrodes are presented. Standard deviations are used to assess the significance of differences between the performances of the catalysts.

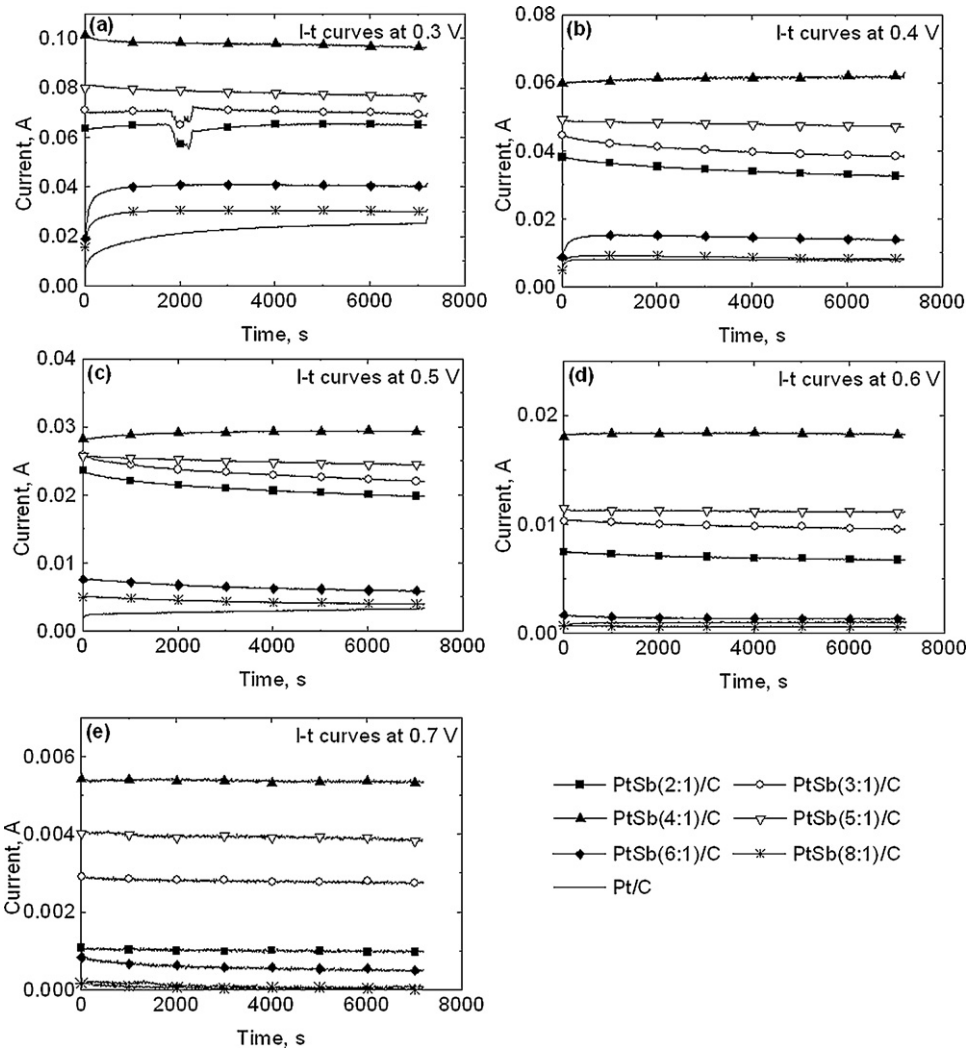

Fig. 5. Average (from three electrodes for each catalyst) current vs. time curves for multi-anode DFAFCs with PtSb(2:1)/C, PtSb(3:1)/C, PtSb(4:1)/C, PtSb(5:1)/C, PtSb(6:1)/C, PtSb(8:1)/C and Pt/C [22] anode catalysts, at cell voltages of 0.3 V, 0.4 V, 0.5 V, 0.6 V and 0.7 V.

Polarization plots (Fig. 4) showed that all of the PtSb/C catalysts gave much better performances than the commercial Pt/C, with PtSb(4:1)/C providing the best performance, with a maximum specific power output of 280 W g^{-1} Pt. In constant cell voltage experiments (Fig. 5), all of the catalysts gave relatively stable performances after ca. 500 s (or less) of operation. The PtSb(4:1)/C catalyst provided the best performance at all cell voltages that were tested. A statistical analysis (*t* test) confirmed that the average currents at the PtSb(4:1)/C electrodes were statistically higher than for any other set of electrodes at the 99.5% confidence level. For the closest case, at +0.5 V, the average current and standard deviation in Fig. 5 was 29.17 ± 0.77 mA for the PtSb(4:1)/C electrodes vs. 24.96 ± 0.88 mA for the PtSb(5:1)/C electrodes.

The superior performance of the PtSb(4:1)/C composition over those with lower Sb contents was presumably due in part to its smaller mean particle size (Table 1). In order to compensate for this, the average currents from the constant cell potential results in Fig. 5 where normalized with respect to the calculated metal surface area of each catalyst, and are plotted against composition in Fig. 6a. It can seen from these data that the surface area effect is relatively small, and that the 4:1 Pt:Sb (0.29 Sb mole fraction) gave the best specific activities. However, its superiority over the 5:1 Pt:Sb (0.24 Sb mole fraction) composition was quite small on this basis.

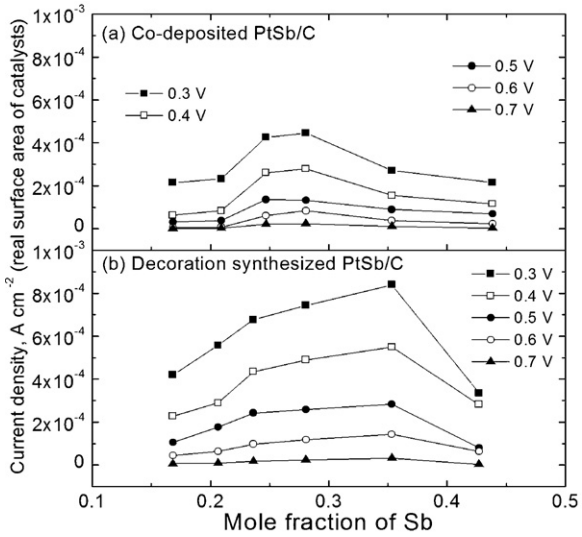

Fig. 6. Average normalized currents for DFAFCs at 0.3 V, 0.4 V, 0.5 V, 0.6 V and 0.7 V with decoration synthesized [22] and codeposited PtSb/C anode catalysts. Currents have been normalized based on Pt (decorated) and PtSb (codeposited) surface areas estimated for spherical particles with radii equal to the mean radii measured by XRD, and weighted average densities for the PtSb particles.

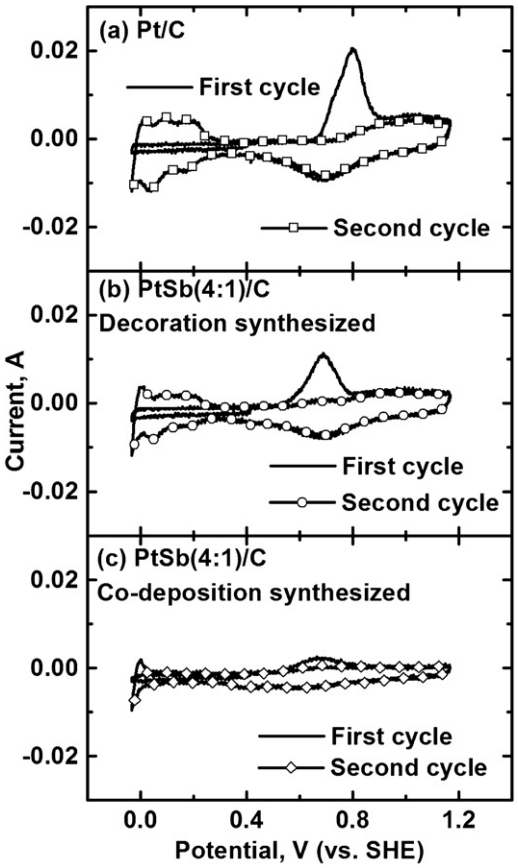

Fig. 7. CO stripping voltammetry (20 mV s^{-1}) in 0.5 M H_2SO_4 of (a) Pt/C, (b) Sb decorated Pt/C with Pt:Sb = 4:1 [22] and (c) codeposited PtSb(4:1)/C. The solid lines are for electrodes that had been exposed to CO for 30 min, while the symbols show the corresponding second cycles.

3.3. CO-stripping

CO-stripping voltammetry of the PtSb(4:1)/C and Pt/C catalysts is shown in Fig. 7. Voltammograms of a previously reported Sb decorated Pt/C catalyst [22] are also presented for comparison. The initial scans in these voltammograms show the voltammetry of the CO poisoned catalyst, while the second cycle shows the voltammogram of the cleaned catalyst following electrochemical oxidation (peak at ca. 0–0.2 V) of the adsorbed CO.

The initial scan for the Pt/C electrode, between −0.2 V and −0.6 V shows complete suppression of the reversible hydrogen adsorption/desorption electrochemistry that is normally seen with Pt, and is indeed seen on the 2nd scan through this region. This indicates that the Pt surface was initially completely covered by strongly adsorbed CO. The peak at ca. +0.2 V on the first anodic scan is due to complete oxidation (stripping) of this CO. The onset of CO oxidation was ca. +0.05 V at the Pt/C electrode.

The codeposited PtSb/C electrode showed very different voltammetric behaviour. The CO stripping peak was very small, and shifted to a lower potential with an onset of ca. −0.05 V. Furthermore, the hydrogen adsorption/desorption peaks seen following CO stripping were very small relative to those seen at the Pt/C electrode. Both of these observations show that the surface of the PtSb(4:1)/C was very unlike a Pt surface. This could be explained by blocking of the Pt rich surface of the alloy particles with a Sb oxide layer, which would be compatible with the XPS results, or a strong electronic effect of Sb(0) atoms in the surface layer of the alloy particles.

In order to help distinguish between blocking and electronic effects, stripping voltammetry was also obtained for Sb decorated Pt/C catalyst (Fig. 7b), for which blocking of the Pt surface by the Sb/Sb oxide layer should be the only effect. In this case, both the CO stripping peak and hydrogen adsorption/desorption peaks were depressed relative to Pt/C, but were much larger than for the codeposited PtSb/C electrode. This implicates the involvement of a strong electronic effect for alloyed Sb for the codeposited PtSb/C.

It can also be seen that the CO stripping peak for the Sb decorated Pt/C catalyst was shifted to lower potentials, relative to Pt/C, to a degree similar to the shift seen for the codeposited PtSb/C. This effect can be attributed to the surface Sb oxide layer, which would promote CO oxidation by the well-known bifunctional mechanism (see below).

4. Discussion

The codeposited PtSb/C catalysts reported here show outstanding performances as anode catalysts for DFAFCs, with the optimum performance seen at a 4:1 Pt:Sb mass ratio (0.29 Sb mole fraction). The XRD, XPS, and CO stripping results show that some of the Sb was alloyed with the Pt, although there also appears to have been a substantial amount of Sb oxide deposited on the surface of the metallic particles. It has previously been shown that similar Sb oxide deposits on Pt promote formic acid oxidation by a bifunctional mechanism in which Sb–OH groups can react electrochemically with CO adsorbed on the Pt sites to produce CO_2, as well as through electronic effects [22]. Comparison of the dependence of the formic acid oxidation activity on the surface coverage of Sb with literature models [28] indicated that there was very little CO poisoning of the Pt surface for the Sb decorated catalysts [22]. This is consistent with reported influence of Sb ad-atoms on CO adsorption and formic acid oxidation at Pt(1 0 0) and Pt(1 1 1), in which the Sb atoms inhibited the adsorption of CO and promoted the dissociation of formic acid [29]. A recent surface-enhanced infrared absorption spectroscopy study has shown that surface Sb decreases the amounts of CO and formate surface species [3]. Coupled with DTF calculations, this indicates that formic acid oxidation at Pt/Sb surfaces occurs largely via a direct pathway involving adsorption of formic acid in a CH-down configuration.

The similarities of the XPS spectra for the codeposited PtSb(4:1)/C catalyst reported here and the previously reported Sb decorated Pt/C catalyst (see Figs. 2 and 3) indicates that subtle differences in structures and composition of PtSb/C catalysts can have profound effects on their electrochemistry. This is particularly apparent in Fig. 7 where the voltammetry of the two seemingly similar PtSb/C catalysts is very different. It is also reflected in the fuel cell performances summarized in Fig. 6, which show average currents at various potential vs. composition for the set of codeposited catalysts reported here and the set of Sb decorated Pt/C catalysts that were previously reported [22]. It is clear from these data that while the two sets of catalysts showed similar dependences of their activity on composition, the decorated catalysts were somewhat more active on a real surface area basis than the codeposited catalysts. Thus although partial alloying of the Sb with Pt in the codeposited catalysts leads to further suppression of CO adsorption, this appears to be offset by the consequent reduction in Pt surface area available for formic acid oxidation.

A rigorous comparison of the activities of the two types of catalyst is complicated by the reported particle size dependence of formic acid oxidation at Pt nanoparticles [30]. It was found that the specific activities of particles with diameters below 4 nm were higher than for larger particles and bulk Pt. This was attributed to a decrease in the availability of the contiguous Pt terrace sites required for formation of CO (ensemble effect), which poisons the Pt surface. The contribution of this effect in the case of PtSn catalysts in unknown, and certainly debatable. Most likely, it will be

much less significant than at pure Pt since Sn strongly inhibits CO formation via its electronic effect (and would also exert its own ensemble effect).

Although this study appears to indicate that Sb decorated Pt/C catalysts are fundamentally superior to codeposited PtSb/C catalyst, because of their higher activities on a real surface area basis, an important practical feature of the codeposition method is the low particle sizes that were achieved. The best codeposited PtSb/C catalyst had a mean PtSb particle size of 1.8 nm, while the commercial Pt/C catalyst used to prepare the decorated catalysts had a Pt particle size of 3.2 nm. Consequently, the codeposited catalyst provided superior fuel cell performances at the same catalyst loading, and on a Pt mass basis. For example, the codeposited PtSb(4:1) catalyst provided a current of 80 mA cm^{-2} at 0.6 V in Fig. 6, with 0.43 mg Pt cm^{-2} while the best decorated catalyst provided only 56 mA cm^{-2} under the same conditions with 0.45 mg Pt cm^{-2} [22]. These results indicate that it should be possible to further improve the performances of PtSb/C catalysts by decreasing the particle sizes of catalysts prepared by decoration of Pt/C.

5. Conclusions

PtSb/C anode catalysts synthesized by codeposition of Pt and Sb on Vulcan® carbon black provide much higher DFAFC performances than Pt/C and are also generally superior, on a Pt mass basis, to similar catalysts prepared by the decoration of Pt/C with Sb. Although the decorated catalysts provided superior formic acid oxidation activities on a surface area basis, this was more than offset by the smaller particle sizes achieved by codeposition. The optimum compositions of both types of PtSb/C catalyst were similar, and the Sb was largely present as a surface oxide in both cases. However, XRD, XPS and CO stripping voltammetry showed that there were substantial differences in the structures of the two types of catalyst. In particular, XRD showed evidence of alloying in the case of the codeposited catalysts and voltammetry revealed a strong suppression of both H and CO adsorption. This suggests that there was a strong electronic effect of alloyed Sb on the properties of the codeposited catalysts that is not present for the decorated catalysts.

Acknowledgements

This work was supported by the Natural Sciences and Engineering Research Council of Canada (NSERC) through a Strategic Projects Grant in partnership with Tekion (Canada) Inc. and by Memorial University. We thank Dr. Zeynel Bayindir (Dalhousie University) for collection and analysis of the XPS data.

References

[1] X. Yu, P.G. Pickup, J. Power Sources 177 (2008) 124.
[2] J.M. Feliu, E. Herrero, in: W. Vielstich, H.A. Gasteiger, A. Lamm (Eds.), Handbook of Fuel Cells, vol. 2, Wiley, New York, 2003, p. 679.
[3] B. Peng, H.F. Wang, Z.P. Liu, W.B. Cai, J. Phys. Chem. C 114 (2010) 3102.
[4] J. Wang, P. Holt-Hindle, D. MacDonald, D.F. Thomas, A. Chen, Electrochim. Acta 53 (2008) 6944.
[5] C. Rice, S. Ha, R.I. Masel, A. Wieckowski, J. Power Sources 115 (2003) 229.
[6] J.H. Choi, K.J. Jeong, Y. Dong, J. Han, T.H. Lim, J.S. Lee, Y.E. Sung, J. Power Sources 163 (2006) 71.
[7] A.V. Tripkovic, S.L. Gojkovic, K.D. Popovic, J.D. Lovic, A. Kowal, Electrochim. Acta 53 (2007) 887.
[8] P. Waszczuk, T.M. Barnard, C. Rice, R.I. Masel, A. Wieckowski, Electrochem. Commun. 4 (2002) 599.
[9] F.S. Thomas, R.I. Masel, Surf. Sci. 573 (2004) 169.
[10] E. Herrero, A. Fernandez-Vega, J.M. Feliu, A. Aldez, J. Electroanal. Chem. 350 (1993) 73.
[11] E. Casado-Rivera, D.J. Volpe, L. Alden, C. Lind, C. Downie, T. Vazquez-Alvarez, A.C.D. Angelo, F.J. DiSalvo, H.D. Abruna, J. Am. Chem. Soc. 126 (2004) 4043.
[12] D. Volpe, E. Casado-Rivera, L. Alden, C. Lind, K. Hagerdon, C. Downie, C. Korzeniewski, F.J. DiSalvo, H.D. Abruna, J. Electrochem. Soc. 151 (2004) A971.
[13] A.V. Tripkovic, K.D. Popovic, R.M. Stevanovic, R. Socha, A. Kowal, Electrochem. Commun. 8 (2006) 1492.
[14] M.D. Macia, E. Herrero, J.M. Feliu, J. Electroanal. Chem. 554 (2003) 25.
[15] S.Y. Uhm, S.T. Chung, J.Y. Lee, Electrochem. Commun. 9 (2007) 2027.
[16] Z.L. Liu, B. Guo, S.W. Tay, L. Hong, X.H. Zhang, J. Power Sources 184 (2008) 16.
[17] L.R. Alden, D.K. Han, F. Matsumoto, H.D. Abruna, F.J. DiSalvo, Chem. Mater. 18 (2006) 5591.
[18] L.R. Alden, C. Roychowdhury, F. Matsumoto, D.K. Han, V.B. Zeldovich, H.D. Abruna, F.J. DiSalvo, Langmuir 22 (2006) 10465.
[19] L.J. Zhang, Z.Y. Wang, D.G. Xia, J. Alloys Compd. 426 (2006) 268.
[20] F. Matsumoto, C. Roychowdhury, F.J. DiSalvo, H.D. Abruna, J. Electrochem. Soc. 155 (2008) B148.
[21] X. Yu, P.G. Pickup, J. Int. Green Energy 6 (2009) 571.
[22] X. Yu, P.G. Pickup, Electrochim. Acta 55 (2010) 7354.
[23] E. Herrero, J.M. Feliu, A. Aldaz, J. Electroanal. Chem. 368 (1994) 101.
[24] J.K. Lee, H. Jeon, S. Uhm, J. Lee, Electrochim. Acta 53 (2008) 6089.
[25] B. Peng, J.Y. Wang, H.X. Zhang, Y.H. Lin, W.B. Cai, Electrochem. Commun. 11 (2009) 831.
[26] X. Yu, P.G. Pickup, J. Power Sources 187 (2009) 493.
[27] I.D. Choi, H. Lee, Y.-B. Shim, D. Lee, Langmuir 26 (2010) 11212.
[28] E. Leiva, T. Iwasita, E. Herrero, J.M. Feliu, Langmuir 13 (1997) 6287.
[29] N. Kizhakevariam, M.J. Weaver, Surf. Sci. 310 (1994) 183.
[30] S. Park, Y. Xie, M.J. Weaver, Langmuir 18 (2002) 5792.